Surface Oscillations in Overdense Plasmas Irradiated by Ultrashort Laser Pulses

A. Macchi,[1,*] F. Cornolti,[1] F. Pegoraro,[1] T. V. Liseikina,[1] H. Ruhl,[2] and V. A. Vshivkov[3]

[1]*Dipartimento di Fisica and INFM (Sezione A), Universitá di Pisa, Pisa, Italy*

[2]*Max-Born Institut, Berlin, Germany*

[3]*Institute of Computational Technologies of SD-RAS, Novosibirsk, Russia*

(Received 5 May 2001; published 29 October 2001)

The generation of electron surface oscillations in overdense plasmas irradiated at normal incidence by an intense laser pulse is investigated. Two-dimensional (2D) particle-in-cell simulations show a transition from a planar, electrostatic oscillation at 2ω, with ω the laser frequency, to a 2D electromagnetic oscillation at frequency ω and wave vector $k > \omega/c$. A new electron parametric instability, involving the decay of a 1D electrostatic oscillation into two surface waves, is introduced to explain the basic features of the 2D oscillations. This effect leads to the rippling of the plasma surface within a few laser cycles, and is likely to have a strong impact on laser interaction with solid targets.

DOI: 10.1103/PhysRevLett.87.205004 PACS numbers: 52.38.Dx, 52.35.Mw, 52.65.–y

The interaction of subpicosecond, high-intensity laser pulses with solid targets is of great relevance to the generation of bright sources of energetic radiation as well as a test bed for fast ignitor physics. Since for a solid target the electron density $n_e \gg n_c$, where $n_c = 1.1 \times 10^{21}\ \mathrm{cm}^{-3}/(\lambda/\mu\mathrm{m})^2$ is the cutoff density for laser propagation at the wavelength λ, the laser-plasma coupling occurs at the target surface over a narrow region with a depth of the order of the skin length $d_p \ll \lambda$. The laser force on the plasma has both secular components (leading to plasma acceleration, profile steepening, and hole boring) and oscillating components; these latter drive an oscillatory motion of the "critical" surface where $n_e = n_c$, which acts as a "moving mirror" leading to the appearance of high harmonics in the reflected light [1].

Experiments [2] and simulations [3–5] suggest that either preimposed or selfgenerated deformations of the target surface strongly affect laser energy absorption. Evidence for small-scale deformations comes from the wide spreading of the reflected radiation observed in experiments [6–8] at high intensities ($\approx 10^{18}\ \mathrm{W\,cm}^{-2}$) and even for pulse durations as short as 35 fs [7]. This suggests that surface rippling involves some "fast" mechanism related to electron motion rather than Rayleigh-Taylor-like (RT) hydrodynamic instabilities driven by the strong target acceleration and occurring on time scales of the ion motion. Seeding of density "ripples" by electron instabilities in the underdense plasma region in front of the target was evidenced in simulations [3] and investigated theoretically in [9].

In this Letter, we show with numerical simulations that electron surface oscillations (ESOs) may grow for a step density profile (no underdense region present) much faster than the typical time scale of ion motion, leading to an oscillatory "rippling" of the critical surface. To interpret the simulations we present a model for a new parametric instability, based on the "decay" of pumped one-dimensional (1D) electrostatic oscillations into two electron surface waves. This represents a new nonlinear mechanism of surface wave excitation by laser pulses different from previously investigated models [10]. Its potentially strong impact on the disruption of "moving mirrors" for high harmonic generation (HHG) and the production of fast electron jets are discussed.

We use two-dimensional (2D) particle-in-cell (PIC) simulations to study the dynamics of the ESOs with proper spatial and temporal resolution. In particular, in order to evaluate the frequency of the ESOs, the complete output of 2D fields was produced eight times for each laser cycle. In the simulations reported, the laser pulse is normally incident, impinges from the left on the x axis, and has a wavelength $\lambda = 0.25\ \mu\mathrm{m}$ ($n_c = 1.6 \times 10^{22}\ \mathrm{cm}^{-3}$), a uniform spatial profile in the transverse (y) direction, and a temporal profile that rises for three cycles and then remains constant. The laser pulse is "s polarized," i.e., its electric field is in the z direction normal to the simulation plane. The plasma has immobile ions, initial temperature $T_e = 5$ keV and a steplike density profile filling the right part of the box ($x > 0$) A numerical box $12\lambda \times 4\lambda$ is taken with a spatial resolution equal to the Debye length $\lambda_D = \sqrt{T_e/4\pi n_o e^2}$, where n_o is the initial density, and 25 particles per cell are used. We will focus on two typical simulations (run 1 and run 2). Introducing the dimensionless irradiance $a_o = 0.85(I\lambda^2/10^{18}\ \mathrm{W}\,\mu\mathrm{m}^2/\mathrm{cm}^2)^{1/2}$ in run 1, we take $a_o = 1.7$ and $n_o = 5n_c$, while in run 2 we take $a_o = 0.85$ and $n_o = 3n_c$.

The contours of the electron density $n_e(x, y)$ in Fig. 1 for run 1 at times $t = 8$, 10, 12, and 14 laser cycles from the run start, show the evolution of the surface dynamics over several laser cycles. Correspondingly, the space-time contours of $n_e(x, y = y_i, t)$ at $y_1 = 2.0\lambda$ and $y_2 = 1.875\lambda$ in Fig. 2 show the temporal behavior of the surface oscillations. Initially, the surface oscillation is planar, i.e., uniform along y, and has a frequency 2ω, being $\omega = 2\pi c/\lambda$ the laser frequency. It is natural to identify this 1D motion as the moving mirror driven by the longitudinal $\mathbf{j} \times \mathbf{B}$ force at 2ω. In the compression phase, electrons pile up in a narrow layer, where the peak density is $n_e \simeq 2n_0$; the

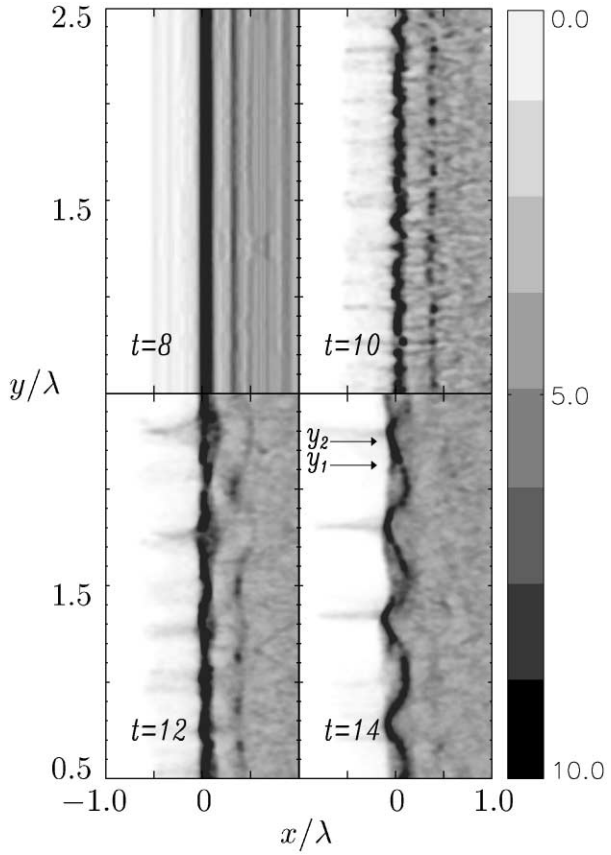

FIG. 1. Contours of normalized electron density n_e/n_c for run 1 ($a_o = 1.7$, $n_o = 5n_c$) at various times (see plot labels) in laser cycle units. Only a small portion of the simulation box around the target surface is shown.

electrostatic field $E_x^{(2\omega)}$ (not shown) is positive and counteracts the $\mathbf{j} \times \mathbf{B}$ force. In the expansion phase electrons are dragged out into vacuum, forming a "cloud" of negative charge with a negative electrostatic field.

The growth of surface ripples can be observed in Fig. 1. At $t = 10$, they have small wavelengths ($\simeq 0.1\lambda$), while at $t \geq 12$ they evolve into a steady oscillation with wavelength $\lambda_s \simeq 0.5\lambda$ (Fig. 1) and frequency $\simeq \omega$, which is superimposed on the oscillation at 2ω (Fig. 2). This "period doubling" effect is also observed in run 2, for which the density contours at $t = 16.5$, 17, 17.5, and 18.0 are shown in Fig. 3: it is evident that the curvature of the density layer is inverted at each half laser cycle. In run 2 the oscillation amplitude and the density compression is lower than in run 1, and the deformation wavelength is larger ($\lambda_s \simeq 0.75\lambda$). In the following we will discuss only the long-wavelength structures oscillating at ω and refer to them as (2D)ESOs. The 2DESOs are "standing," i.e., not propagating along y. From Fig. 2 we see that, while at y_1 the amplitude is close to its maximum, at $y_2 = y_1 - \lambda_s/4$ there is no evident growth of the oscillation at ω, while a weakening of the 2ω oscillation is observed. Results (not shown) for p polarization at normal incidence (i.e., with the electric field of the laser pulse in the y direction) are qualitatively similar, the main difference being that the plasma "plumes" extending into vacuum are bent by the laser field in the plane.

To our knowledge, there are no previous simulations or models describing surface ripples of the electron density oscillating at the laser frequency for normal incidence. In the moving mirror motion a superposition of ω and 2ω motions occurs only for oblique incidence and p polarization, because in such a case both the electric and magnetic forces have components normal to the surface [11]. In Ref. [12] grating-like surface inhomogeneities oscillating at 2ω and induced by the magnetic force at oblique incidence were studied. Stationary surface ripples in the ion density were observed in simulations [9] at much longer times [13] and interpreted on the basis of a hydrodynamic model for an underdense, homogeneous, neutral plasma which leads (for s polarization only) to an instability pumped by the secular part of the ponderomotive force. Our explanation is that the 2DESOs are generated by a parametric decay of the forced 1D oscillation with frequency 2ω and transverse wavevector $k_y = 0$ into two electron surface waves (ESWs) (ω_1, k_1) and (ω_2, k_2). Using the matching conditions $k_1 + k_2 = 0$ and $\omega_1 + \omega_2 = 2\omega$ we find that the two overlapping ESWs thus form

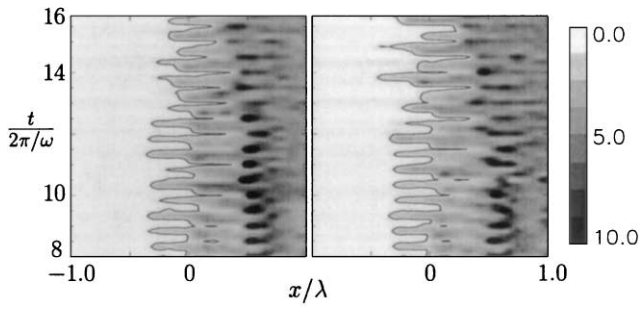

FIG. 2. Space-time evolution of $n_e(x, y = y_l, t)$ at $y_1 = 1.875/\lambda$ (left) and $y_2 = 2.0\lambda$ (right) for run 1 (see Fig. 1). The position of the $n_e = n_c$ surface is evidenced by a black contour line.

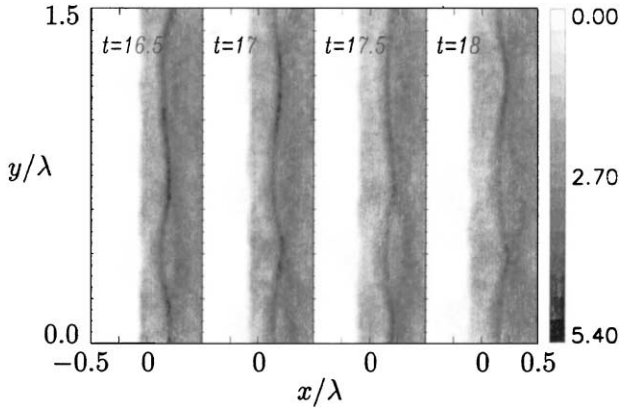

FIG. 3. Same as Fig. 1 for run 2 ($a_o = 0.85$, $n_o = 3n_c$).

a standing oscillation with frequency $\omega = \omega_1 = \omega_2$ and wave vector $k = k_1 = -k_2$.

A cold fluid, nonrelativistic 2D model of the parametric excitation of ESWs has been developed. Here we report only a brief description of this model while a detailed derivation will be published elsewhere [14]. The quiver motion along z is solved and a system of 2D Maxwell-Euler equations is obtained, where the laser action enters via the ponderomotive force. The electron fluid density and velocity are written as $n_e = n_o(x) + \epsilon \delta n_e^{(2\omega)}(x,t) + \epsilon^2 \delta n_e^{(\omega)}(x,y,t)$ and $\mathbf{v}_e = \epsilon V_x^{(2\omega)}(x,t)\hat{\mathbf{x}} + \epsilon^2 \mathbf{v}^{(\omega)}(x,y,t)$, where $\epsilon \sim a_o^2(n_c/n_e)$ is a small expansion parameter. The terms at 2ω describe the electrostatic, 1D moving mirror oscillation, which acts as a pump for the instability, and is assumed to be unperturbed by the ESWs. The terms at ω are the superposition of two ESWs:

$$\mathbf{v}^{(\omega)} = e^{-i\omega t}(\tilde{\mathbf{v}}_{+k} e^{iky} + \tilde{\mathbf{v}}_{-k} e^{-iky})/2 + \text{c.c.}, \quad (1)$$

where $\tilde{\mathbf{v}}_{\pm k} = \tilde{\mathbf{v}}_{\pm k}(x,t)$ varies slowly in time. To order ϵ^2, the coupling between 1D and 2D modes may be neglected, so that one obtains the usual dispersion relation for "H" surface waves propagating along a density discontinuity:

$$k^2 c^2 = \omega^2(\omega_p^2 - \omega^2)/(\omega_p^2 - 2\omega^2), \quad (2)$$

where $\omega_p^2 = 4\pi n_o e^2/m_e$ is the plasma frequency. The evanescence length of the ESWs in the plasma is $L_{SW} = (c/\omega)(1 - 2\omega^2/\omega_p^2)^{1/4}(1 - \omega^2/\omega_p^2)^{-1/2}$. Notice that for electron surface waves $\nabla \cdot \mathbf{E}^{(\omega)} = -4\pi e \delta n_e^{(\omega)}(x,y,t) = 0$, and that their maximum frequency is $\omega_{\max} = \omega_p/\sqrt{2}$, so that the matching conditions may be satisfied only if $\omega < 2\omega_{\max}$, i.e., $n_e > 2n_c$.

By inserting the value of the laser frequency in (2), we find that the expected wavelength of deformations in run 2 is $\lambda_s = 2\pi/k \simeq 0.71\lambda$, in good agreement with the simulation. For run 1, one finds $\lambda_s \simeq 0.87\lambda$, much larger than the numerical result. This is not surprising since our expansion procedure is not applicable for the parameters of run 1, where the interaction is in the relativistic regime. This may cause, for instance, a lowering of the effective plasma frequency by the (time-averaged) relativistic factor $\gamma_o \simeq \sqrt{1 + a_o^2/2}$, mostly due to the relativistic quiver motion along z. By replacing ω_p^2 by ω_p^2/γ_o in (2), for run 1 we obtain $\lambda_s \simeq 0.55\lambda$, much closer to the numerical result.

By keeping only terms of order ϵ^3 in the Euler equation and neglecting feedback effects on the 1D motion, the Euler equation for the ESW velocity is $\partial_t \mathbf{v}^{(\omega)} = -e\mathbf{E}^{(\omega)}/m_e + \epsilon \mathbf{a}_{NL}^{(\omega)}$ where $\mathbf{a}_{NL}^{(\omega)}$ describes the nonlinear coupling with the 1D motion:

$$\mathbf{a}_{NL}^{(\omega)} = -V_x^{(2\omega)} \partial_x \mathbf{v}^{(\omega)} - v_x^{(\omega)} \partial_x V_x^{(2\omega)} \hat{\mathbf{x}} + \frac{e V_x^{(2\omega)}}{m_e c} B_z^{(\omega)} \hat{\mathbf{y}}. \quad (3)$$

Using this equation and Poynting's theorem the rate of growth of the surface energy for the 2DESOs was evaluated as $\Gamma \equiv U^{-1} \partial_t U$, where U is the energy density per wavelength of the two ESWs and the cycle-averaged variation is

$$\partial_t U = \int dx \langle \mathbf{v}^{(\omega)} \cdot (e \delta \tilde{n}_e^{(2\omega)} \tilde{\mathbf{E}}^{(\omega)} + m_e n_o \partial_t \tilde{\mathbf{v}}^{(\omega)}) \rangle$$
$$= \frac{1}{4} \int_0^{+\infty} dx\, \tilde{\mathbf{v}}_{+k}^* \cdot \left(e \delta \tilde{n}_e^{(2\omega)} \tilde{\mathbf{E}}_{-k}^* - m_e n_o \tilde{v}_{x,-k}^* \partial_x V_x^{(2\omega)} - m_e n_o \tilde{V}_x^{(2\omega)} \partial_x \tilde{\mathbf{v}}_{-k}^* + n_o \frac{e}{c} \tilde{V}_x^{(2\omega)} \tilde{B}_{z,-k}^* \hat{\mathbf{y}} \right) + \text{c.c.} \quad (4)$$

Substituting in the integrand for the expressions of the (unperturbed) ESW fields, one finally obtains the growth rate as

$$\Gamma \simeq 4\omega a_o^2 \frac{(\alpha - 1)^{3/2}}{\alpha|\alpha - 4|[(\alpha - 1)^2 + 1](\alpha - 2)^{1/2}}, \quad (5)$$

where $\alpha = n_e/n_c = \omega_p^2/\omega^2$. The denominator $(\alpha - 4)$ is actually due to the resonant excitation of longitudinal plasmons at $\omega_p = 2\omega$, which makes $V_x^{(2\omega)}$ very large and invalidates our ordering assumptions near resonance. We note that Γ also diverges for $\alpha \to 2$; however, in this limit the ESW wavelength is very small and thus one expects a strong damping by thermal effects neglected in the cold fluid model.

Our model is valid at normal incidence for both s and p polarizations (in the sense of the 2D simulations), since even if the laser electric field is parallel to the k vectors of the ESWs there is no resonant coupling of the quiver motion with the ESWs. The transverse oscillations are, however, observed more clearly for s rather than for p polarization, since in the latter case the motions in the laser and the ESW fields overlap in the polarization plane. For oblique incidence and p polarization, in addition to the 2ω motion, the laser drives the moving mirror at frequency ω, which may lead to the pumping of two ESW sidebands around the frequency $\omega/2$ [15]. This latter case is directly relevant to experiments on HHG, where the surface rippling observed at high intensities may pose a limit to HHG as an efficient XUV source. The normal incidence results already indicate their potential relevance to the interpretation of this phenomenon. The growth rate is maximum in conditions "optimal" for HHG, i.e., when the moving mirror oscillation is driven at high velocities, which requires a moderate density "shelf" rather than solid densities. In these conditions, at the time of maximum pulse intensity the plasma has a finite gradient at the surface $n_e = n_c$ which is in turn steepened by the radiation pressure. Therefore, the plasma profile may

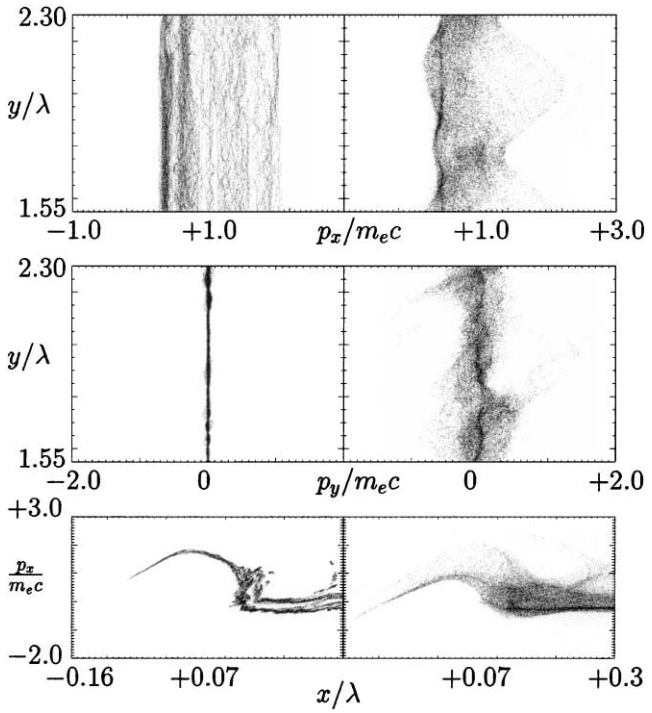

FIG. 4. Phase space projections for run 1 in the (y, p_x) (top), (y, p_y) (middle), and (x, p_x) (bottom) planes for $t = 8.5$ (left) and $t = 13.5$ (right) laser cycles.

look rather similar to that assumed in our simulations. In such conditions the ESO instability can be much faster than RT instabilities. In fact, even for accelerations of order $g \simeq 10^{20}$ cm/s^2 as measured in this regime [16], the typical RT growth rate $\Gamma_{\mathrm{RT}} \simeq \sqrt{k_{\mathrm{RT}} g} \simeq (140\ \mathrm{fs})^{-1}$ for $2\pi/k_{\mathrm{RT}} \simeq \lambda/2 = 0.125\ \mu$m, is much slower than the rise of the 2DESOs which occurs over a few fs in the simulations.

Finally, the results of run 1 give an indication of the scaling of the growth rate in the relativistic regime, not accessible to our analytical model; the growth rate may increase strongly for relativistic intensities due to the decrease of the effective plasma frequency, producing a stronger rippling of the surface, consistent with the simulation results and experiments that suggest that the instability threshold is close to $a_o = 1$.

The ESOs also have a substantial impact on fast electron generation. Figure 4 shows phase space distributions at times $t = 8.5$ and 13.5 laser cycles for run 1. At early times, the momentum distribution is uniform in y, with no accelerated particles in p_y and most energetic electrons having $p_x \simeq 2m_ec$. At later times, when the 2DESOs have grown, stronger forward acceleration occurs near the maxima of the oscillation, showing that most oscillatory energy has been transferred to the unstable 2D modes. Correspondingly, strong acceleration in p_y also occurs. The momentum distribution in p_x is very regular, with only a minority of electrons "outrunning" the oscillation. This suggests that the generation of fast electrons is correlated with the nonlinear evolution and "breaking" of the density oscillations, when the amplitude of the latter exceeds the screening length. This may give a spatial "imprint" on the transverse structure of the fast electron currents. In previous simulations, one may clearly observe a spatial correlation between electron jets and "corrugations" at the surface [17,18]. When penetrating into the bulk the jets may either merge or drive current filamentation instabilities [18,19], thus producing different spatial scales.

The PIC simulations were performed at the CINECA Supercomputing Facility (Bologna, Italy), sponsored by the INFM Supercomputing Initiative.

*Electronic address: macchi@df.unipi.it

[1] S. V. Bulanov, N. M. Naumova, and F. Pegoraro, Phys. Plasmas **1**, 745 (1994).
[2] T. Feurer *et al.,* Phys. Rev. E **56**, 4608 (1997).
[3] S. C. Wilks *et al.,* Phys. Rev. Lett. **69**, 1383 (1992).
[4] H. Ruhl *et al.,* Phys. Rev. Lett. **82**, 2095 (1999).
[5] A. Macchi, H. Ruhl, and F. Cornolti, Laser Part. Beams **18**, 375 (2000).
[6] P. A. Norreys *et al.,* Phys. Rev. Lett. **76**, 1832 (1996); M. Zepf *et al.,* Phys. Rev. E **58**, R5253 (1998).
[7] A. Tarasevitch *et al.,* Phys. Rev. E **62**, 023816 (2000).
[8] C. Dietrich *et al.,* in Proceedings of the Second ULIA conference, Pisa, 2000 (unpublished).
[9] M. G. Cadjan, M. F. Ivanov, and A. V. Ivlev, Phys. Lett. A **222**, 324 (1996); Laser Part. Beams **15**, 33 (1997).
[10] R. Dragila and S. Vukovic, Phys. Rev. Lett. **61**, 2759 (1988); E. G. Gamaliy, Phys. Rev. E **48**, 516 (1993); S. A. Magnitskii, V. T. Platonenko, and A. V. Tarasishin, in *Superstrong Fields in Plasmas,* edited by M. Lontano, G. Mourou, F. Pegoraro, and E. Sindori, AIP Conf. Proc. No. 426 (AIP, New York, 1998), p. 73, and references therein.
[11] D. von der Linde and K. Rzazewski, Appl. Phys. B **63,** 499 (1996).
[12] L. Plaja, L. Roso, and E. Conejero-Jarque, Astrophys. J. Suppl. Ser. **127**, 445 (2000).
[13] In principle, the long time evolution of 2DESOs may lead to ion density ripples similar to those observed in [9], which, however, have a wavelength $\lambda_s > \lambda$, while the opposite inequality holds in our model of 2DESOs based on surface wave excitation.
[14] A. Macchi, F. Cornolti, and F. Pegoraro, physics/0105017.
[15] A. Macchi *et al.,* in "*Superstrong Fields in Plasmas 2,*" edited by M. Lontano (AIP, New York, to be published).
[16] R. Sauerbrey, Phys. Plasmas **3**, 4712 (1996).
[17] B. Lasinski *et al.,* Phys. Plasmas **6**, 2041 (1999).
[18] Y. Sentoku *et al.,* Phys. Plasmas **7**, 689 (2000).
[19] F. Califano *et al.,* Phys. Rev. E **58**, 7837 (1998), and references therein.